



Kinetic and thermodynamic studies on biosorption of Cr(VI) on raw and chemically modified *Datura stramonium* fruit

Shravan Kumar · Tasrin Shahnaz · N. Selvaraju · Prasanna Venkatesh Rajaraman

Received: 29 March 2019 / Accepted: 24 February 2020 / Published online: 23 March 2020
© Springer Nature Switzerland AG 2020

Abstract Biosorption of Cr(VI) on sulfuric and phosphoric acid-treated *Datura stramonium* fruit was investigated in batch mode. The various parameters that influence the biosorption process such as Cr(VI) initial concentration, biosorbent dosage, contact time, temperature, and pH value were optimized. Both linear and non-linear regression analysis of isotherm data suggest that Langmuir isotherm model mimics the behavior of Cr(VI) ion biosorption onto *Datura stramonium* fruit biosorbent. The maximum Cr(VI) ions adsorption capacity of 138.074 mg/g at pH 2 is achieved with

phosphoric acid treated *Datura stramonium* (PDSF). The kinetics of adsorption process is well described by pseudo-second-order model with high R^2 and low χ^2 value. The estimated activation energy of < 8 kJ/mol obtained for both raw and chemically modified adsorbents suggests that the adsorption occurs mainly via physisorption. Besides, thermodynamic results reveal that biosorption of Cr(VI) on both treated and untreated *Datura stramonium* was endothermic, spontaneous, and randomness in nature.

Highlights

- *Datura stramonium* fruit was used as novel biosorbent for the biosorption of Cr(VI).
- The maximum Cr(VI) uptake on RDSF, SDSF, and PDSF biosorbents obtained was found to be 85.916, 119.632, and 138.074 mg/g respectively at optimum pH 2.0.
- The observed free energy (ΔG° (kJ/mol)) values were - 0.249, - 0.026, and - 0.107 for RDSF, PDSF, and SDSF biosorbents respectively.
- The Langmuir isotherm and pseudo-second-order kinetics models mimic the biosorption behavior of Cr(VI).
- The activation energy onto RDSF, SDSF, and PDSF adsorbent was estimated to be 0.192, 7.632, and 7.794 kJ/mol respectively

Keywords Biosorption · Chromium (VI) · Physico-chemical · Thermodynamics · Kinetics · *Datura stramonium*

Introduction

Environmental pollution is the result of rapid urbanization, globalization, industrialization, and unprecedented increment of the population. Water pollution is one of the vital issues that the humanities face today. The emerging economics of the societies in terms of industry, agriculture, and several facilities depend on indispensable resources of water. Pollution is the adverse changes in the environment by the introduction of contaminants as well as of foreign entities. Various industries discharge their effluent without proper treatment into the river stream, in the ocean, and in open land. Discharging of effluents containing heavy metal (metals having specific weight more than 5 g/cm³) from industries is of

S. Kumar · P. V. Rajaraman (✉)
Department of Chemical engineering, Indian Institute of Technology Guwahati, Guwahati, Assam, India
e-mail: rprasanna@iitg.ac.in

T. Shahnaz · N. Selvaraju (✉)
Department of Biosciences and Bioengineering, Indian Institute of Technology Guwahati, Guwahati, Assam, India
e-mail: selva@iitg.ac.in

global concern (Mahmud et al. 2016; Etim et al. 2016). The heavy metals present in the water are a major concern to aquatic and human life due to their toxicity and non-biodegradability nature (Lv et al. 2017). Among the heavy metals, Cr(VI) is commonly used in metal finishing, magnetic tapes, pigments, leather tanning, and electroplating industries (Barakat 2011). Chromium is found in several oxidation states among which Cr(VI) is highly dangerous.

Excessive exposure or intake of Cr(VI) heavy metal more than the permissible limit would cause severe health disorders such as weight loss, cancer, kidney, and liver malfunction (Yogeshwaran and Ak 2017). Therefore, treatment of wastewater is very essential before discharging into the environment. The task of removing Cr(VI) from wastewater have drawn the attention of many researchers and scientists towards development of low-cost and energy-efficient technology, although many conventional methods have been adopted to treat the wastewater. The removal of heavy metal from wastewater is accomplished by several methods including ion exchange, membrane filtration, precipitation, and adsorption (Barakat 2011). However, the adsorption process is relatively easy in operation, recyclable, and a low-cost operative technique in comparison to other conventional methods (Ma et al. 2018). Several types of adsorbents have been investigated by researchers such as zeolite, industrial byproduct, agricultural waste, polymeric material, and plant- and microbial-based biomass for Cr(VI) biosorption. In recent years, agricultural waste adsorbents have been used in biosorption process since it produce the less sludge and also it is recyclable (Abdel-Ghani et al. 2008). Several low-cost agricultural waste biosorbents were reported in the literature such as apple residue (Ho Lee et al. 1998), sawdust (Shukla et al. 2005), grainless stalk of corn (Bellu et al. 2008), waste tea (Ahluwalia and Goyal 2005), wheat bran (Nameni et al. 2008), peanut husk (Olguin et al. 2013), rice husk (Sugashini and Begum 2013), *Citrus limetta* peel (Saha et al. 2013), and *Caryota urens* (Rangabhashiyam and Selvaraju 2015a, 2015b) for removing the heavy metal ions from wastewater. However, finding a low-cost and environmental friendly biosorbent is still an exciting and challenging job for the environmental researchers.

Materials and method

An agro-based sample, *Datura stramonium* sample, was brought from Assam province, India. The collected sample was washed with tap water followed by distilled water. After washing the sample thoroughly, the sample was kept in an oven at 60 °C until dry weight becomes constant. The dried sample was grounded in a mixer and then screened through standard sieves to obtain the desired size of the sample. This sieved sample was stored in a desiccator for further use. Chemical treatment was carried with H₂SO₄ (98%) in a ratio of 2:1 w/v (acid:biomass) and then the sample was kept at 150 °C in an oven for 24 h to get the sample in carbonized form. In order to neutralize the pH value, distilled water was used to wash the carbonized sample and then it was soaked in 1% NaHCO₃ (w/v) solution. Then the sample was kept in an oven at 105 °C for 24 h after washing with distilled water. Second treatment was carried out by mixing 88% ortho-phosphoric acid with the dried sample in the ratio 1:2.5 w/v (biomass:acid) and followed by drying the sample at 110 °C for 2–3 h. After that, muffle furnace was used to carbonize the sample from room temperature to 400 °C for 1.5 h. Then the sample was soaked overnight in 1% solution of NaHCO₃. Then the sample was washed with distilled water to remove residual acid from the sample and dried at 150 °C for 24 h. Finally, the prepared ortho-phosphoric acid-treated *Datura stramonium* (PDSF) and sulfuric acid-treated *Datura stramonium* (SDSF) were stored separately in airtight container for later use (Singha and Das 2011; Rangabhashiyam and Selvaraju 2015a, 2015b; Nakkeeran and Selvaraju 2017).

Preparation of standard solution

The synthetic standard solution was prepared by adding 2.828 g of K₂Cr₂O₇ in distilled water of 1000 ml. It was then diluted to make the desired strength of adsorbate solution for the experiments. The pH value of the solution was attuned by using 0.01 M NaOH/HCl and a pH meter.

Batch biosorption experiments

Biosorption of Cr(VI) on RDSF (Raw sample), PDSF, and SDSF adsorbents from the simulated wastewater was carried out in batch mode. Batch biosorption experiments were done by varying different factors such as

initial hexavalent Cr concentration, dosage of biosorbent, temperature of solution, contact time, and the pH value of solution. In these experiments, the DS (treated or untreated) biosorbents were added to Cr(VI) solution of desired concentration. Thereafter, it was agitated in an orbital shaker at 100 rpm at a predetermined temperature for 1 h. After attaining the equilibrium, it was strained to separate the adsorbent from supernatant using a filter paper (Whatman no. 42). The leftover Cr(VI) in supernatant was assessed through double-beam UV-visible spectroscopy technique at 540-nm wavelength after complex formation of Cr(VI) with 1,5-diphenylcarbazide in the pH range 2–3. The quantity of Cr(VI) biosorbed at equilibrium time and the percentage removal on adsorbent were found by employing Eqs. (1) and (2) respectively.

$$q_t = \frac{(C_0 - C_t)}{m} \times V \tag{1}$$

$$\%R = \frac{(C_0 - C_t)}{C_0} \times 100 \tag{2}$$

Here, q_t (mg/g) is the quantity biosorbed at equilibrium time, V denotes the volume (L), and the biosorbent weight is represented by m (g). The initial and equilibrium concentration of hexavalent chromium (mg/L) are represented by C_0 and C_t respectively. In data analysis of batch experiments, average values were taken after performing experiments in triplicates.

Modeling of equilibrium isotherm, sorption kinetic, and data fitness

Generally, model parameters are more frequently estimated by linear regression method. However, non-linear regression analysis gives more reliable results (Chen et al. 2008). Thus, in the present study, both linear and non-linear regression analysis were employed to evaluate the model parameters values (isotherm and kinetics model equation). Besides, error calculation analysis were performed to quantify the difference between the experimental data and the predicted by the model.

Non-linear regression analysis

Non-linear regression analysis was performed using the original form of kinetics and isotherm model equations. The best fit model parameters were extracted using an

optimization technique. The main objective function of the optimization is to minimize the χ^2 value described in the Eq. 3. The optimization was carried out by using solver add-in in Microsoft Excel application.

$$\chi^2 = \sum_{i=1}^m \left(\frac{Q_i - q_i}{q_i} \right)^2 \tag{3}$$

where Q_i is the experimentally observed adsorbed concentration, q_i is the predicted amount of adsorbed on adsorbent, and m represents the number of observations carried out in the experiment (Chen et al. 2008).

Results and discussion

Characterization of raw and carbonized activated *Datura stramonium*

FESEM was performed to analyze morphology of the biosorbent and the results are shown in Fig. 1. The FESEM micrograph of RDSF shown in Fig. 1 a revealed that fibers are agglomerated with less pores and less rough surface. The morphology of PDSF (Fig. 1b) revealed the difference in size and shape of pores, and fiber, due to the removal of volatile gases.

The SDSF morphology in Fig. 1c shows that pores are open due to the removal of viscous compound. The FESEM morphologies (Fig. 1d–f) after Cr(VI) adsorption show that the biosorbent surface became smooth due to filling up of Cr(VI) metal ions in pores. Energy-dispersive X-ray (EDX) studies of biosorbent sample were carried out before and after biosorption in order to support the information obtained from FESEM and the results are shown in Fig. 2. The EDX spectra exhibit C and O peaks on the biosorbents surface before biosorption as shown in Fig. 2 (a, b and c). The EDX spectra showed a new peak after biosorption of Cr(VI) (refer to Fig. 2 (d, e and f)) which suggests that it is a characteristic signal of Cr(VI) ion.

FTIR spectra were carried out to obtain an information about the functional groups which involved in binding of Cr(VI) ions. The deviation in vibrational frequency was used to predict the same. FTIR spectrum of biosorbents showed a number of absorption peaks (unloaded and loaded Cr(VI)) in the range 400–4000 cm^{-1} which suggest the complex nature of biosorbents. FTIR spectra of RDSF biosorbent (before

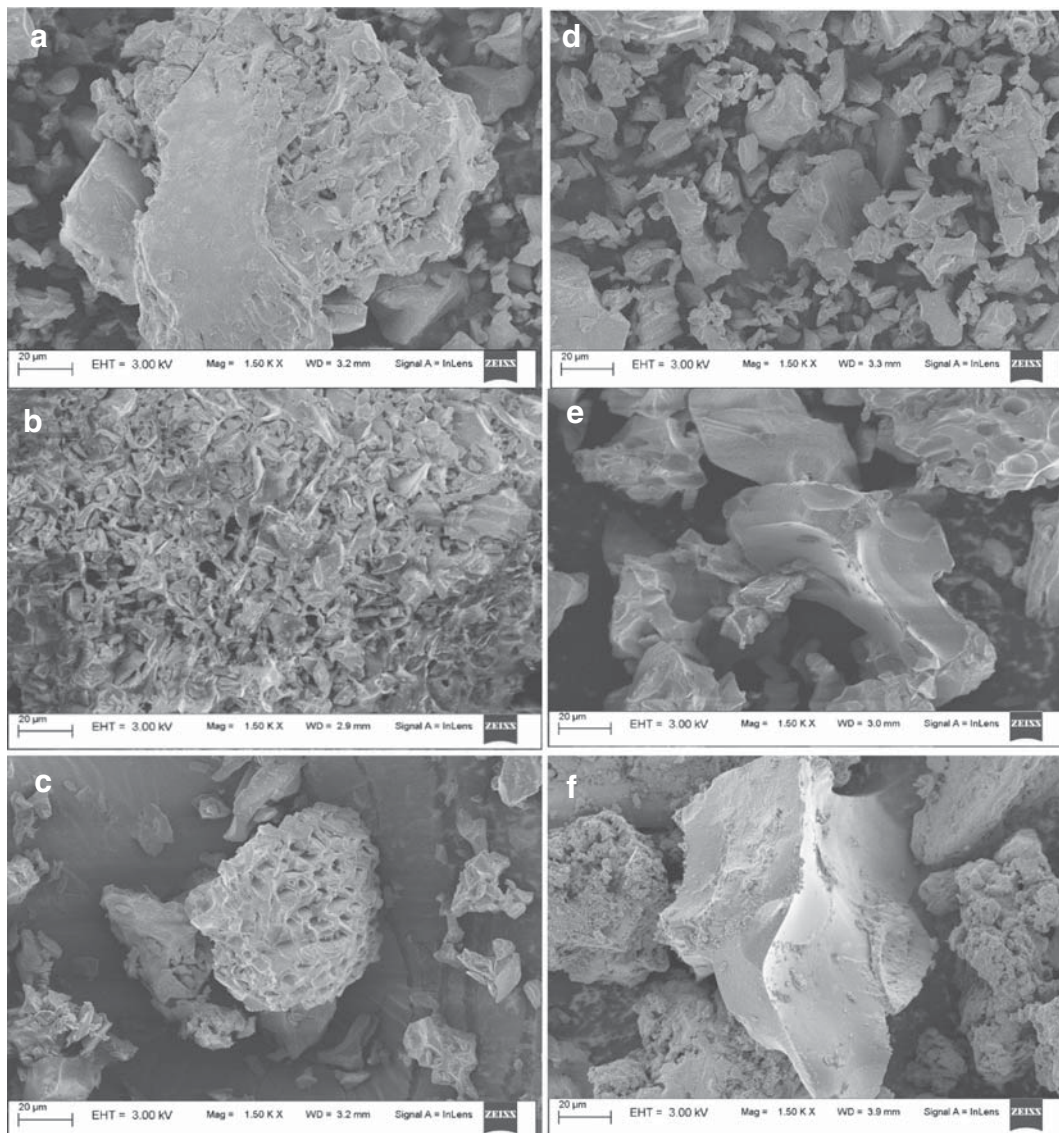


Fig. 1 Scanning electron micrographs of RDSF (a, d), PDSF (b, e), and SDSF (c, f), before and after biosorption

and after biosorption) display several absorption peaks as shown in Fig. 3a. The absorption peaks of unloaded biosorbent assigned at 3655.10, 2893.71, 1737.27, 1523.76, and 1258.86 were shifted to 3566.38, 2884.71, 1728.23, 1513.32, and 1251.63 respectively after biosorption of Cr(VI). These absorption peaks represent O–H stretch, C–O stretch, C–H stretch, C=C, and C=O stretch which contributed to the binding of Cr(VI) ions onto the biosorbent surface. FTIR spectrum of SDSF biosorbent (before and after biosorption) indicates that there is a considerable change in band of functional groups as shown in Fig. 3b. FTIR spectrum peaks after biosorption in contrast to before biosorption

were moved from 3556.20, 1637.63, 1359.69, 1229.29, and 760 to 3529.60, 1511.66, 1341.70, 1226.45, and 751.66 respectively. These adsorption peaks correspond to O–H stretch, N–O stretch, C=O stretch, and C–O functional groups which contributed in binding of Cr(VI) ions with the biosorbent surface.

Similarly, FTIR spectrum of Cr(VI)-loaded PDSF biosorbents reveals the shifting of absorption peaks from 3619.39, 3081.64, 1737.22, 1535.33, and 778.65 to 3584.40, 3064.63, 1710.23, 1502.54, and 751.66 respectively. These absorption peaks represent the functional group such as O–H stretch, C=C stretch, =C–H stretch, and C=O stretch as shown in Fig. 3c. The

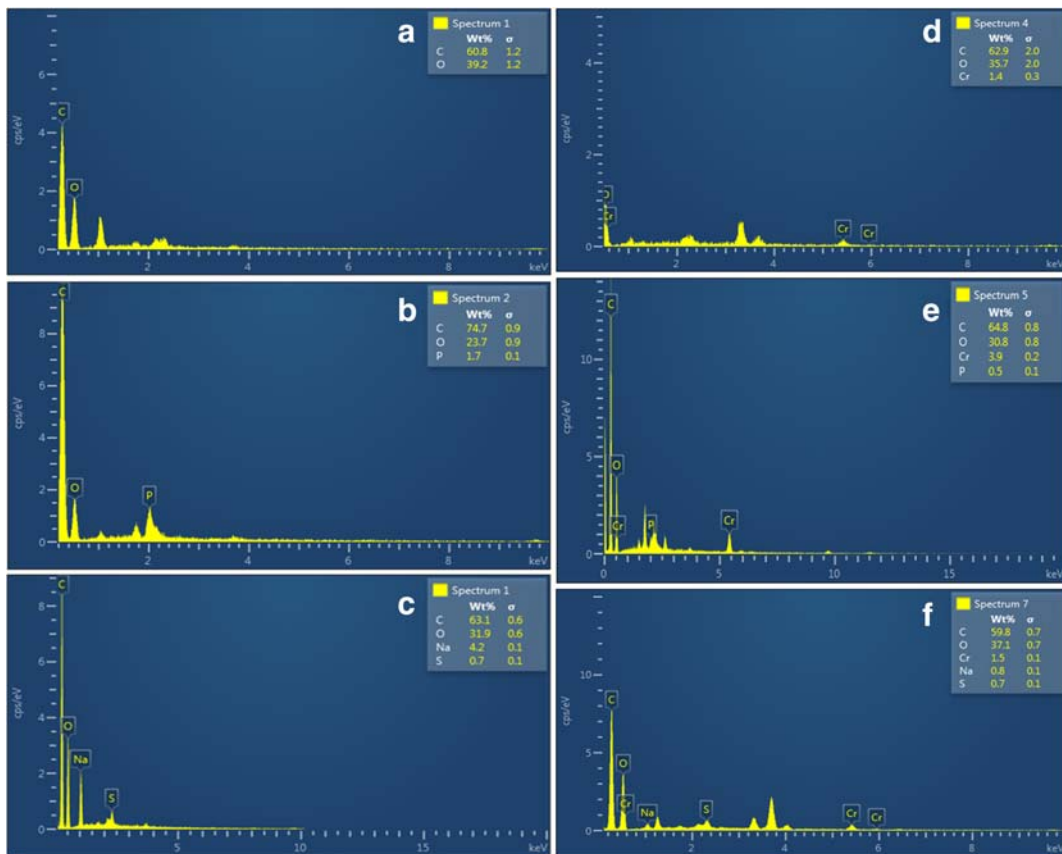


Fig. 2 EDX image of RDSF (a, d), PDSF (b, e), and SDSF (c, f), before and after biosorption

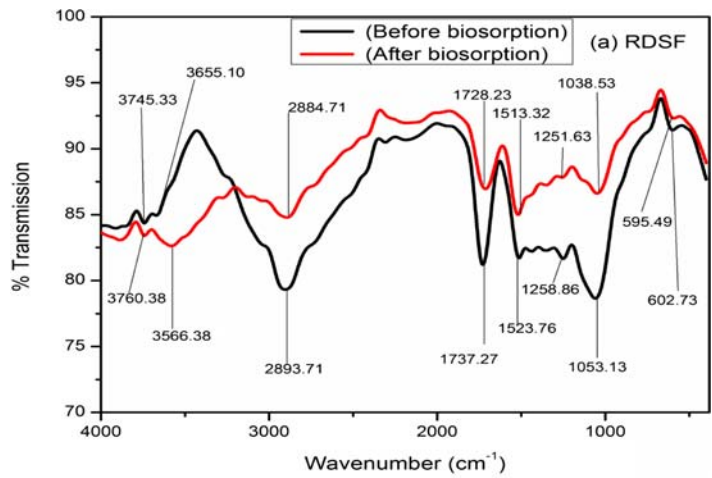
changes in FTIR spectrum from unloaded to loaded Cr(VI) of biosorbents are indicating the fact that the functional groups are indulged in biosorption of Cr(VI). Similar results were presented by other researchers to assess the biosorption of Cr(VI) through functional groups (Singha and Naiya 2011; Jaina et al. 2009).

Influences of pH

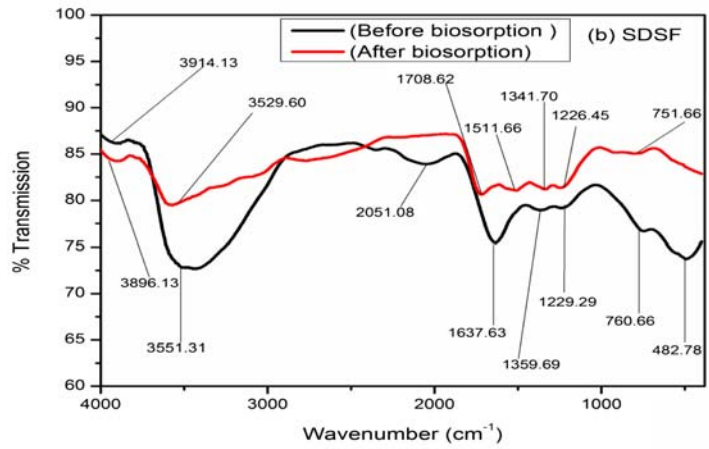
The pH value of the aqueous medium plays an important role in biosorption of Cr(VI) by the biosorbents' surface. In the present study, biosorption experiments were conducted over a wide range of pH from 2 to 9, keeping other parameters as constant. It is revealed from Fig. 4 that uptake capacity of Cr(VI) on RDSF, SDSF, and PDSF biosorbents increases as the pH of the sorbent solution decreases. The estimated biosorption capacity of Cr(VI) was 44.64 mg/g, 50.72 mg/g, and 50.42 mg/g on RDSF, PDSF, and SDSF respectively at pH 2 of the aqueous medium. Biosorption phenomenon of Cr(VI) on RDSF, SDSF, and PDSF can be described by

changes in polarity of the biosorbents' surface due to variation in pH of metal solution. The biomass attains positive charge due to lower pH and gradually gets deprotonated as the pH of the solution rises. Cr(VI) occurs in different ionic forms in the aqueous solution such as chromate (CrO_4^{2-}), dichromate ($\text{Cr}_2\text{O}_7^{2-}$), and hydro chromates (HCrO_4^-) depending upon the pH value of the aqueous medium. HCrO_4^- ions dominate among all the chromate ions at low pH values while CrO_4^{2-} ions dominate towards the higher pH values of the aqueous medium. Biomass gets protonated at lower pH of solution and therefore more biosorption of Cr(VI) takes place at this pH range, due to the electrostatic force of attraction between HCrO_4^- ions and protonated biosorbent surface. At higher pH, the concentration of OH^- increases and therefore biosorption capacity of the biosorbents drop due to the electrostatic force of repulsion between the CrO_4^{2-} and OH^- ions, which causes hindrance in path of chromate ion binding on the active sites of the biosorbent (Rangabhashiyam and Selvaraju 2015a, b; Blazquez et al. 2009).

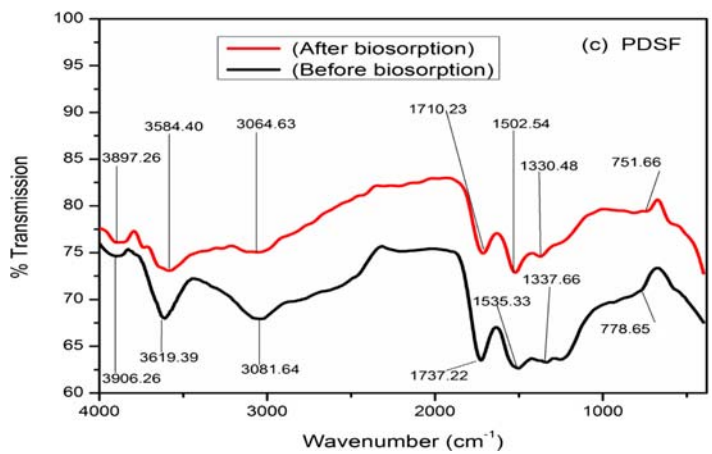
Fig. 3 **a** FTIR spectrum of unloaded and metal-loaded on RDSF biosorbent. **b** FTIR spectrum of unloaded and metal-loaded on SDSF biosorbent. **c** FTIR spectrum of unloaded and metal-loaded on PDSF biosorbent



(a) FTIR spectrum of unloaded and metal-loaded on RDSF biosorbent.

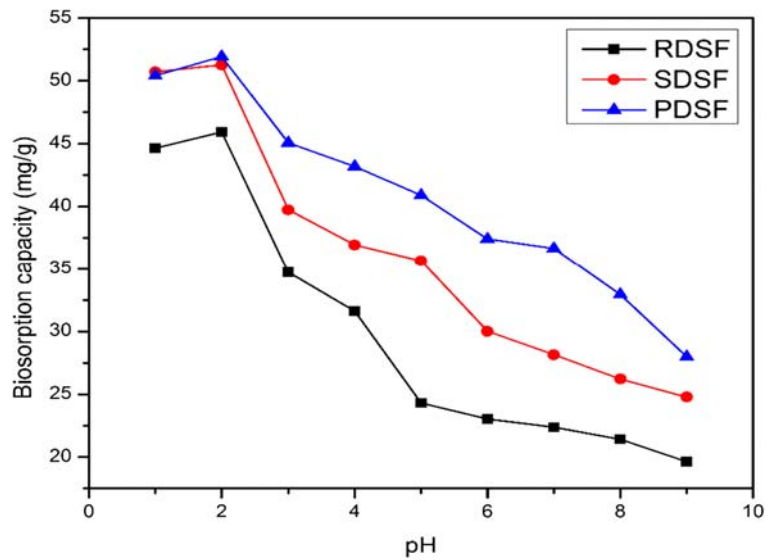


(b) FTIR spectrum of unloaded and metal-loaded on SDSF biosorbent.



(c) FTIR spectrum of unloaded and metal-loaded on PDSF biosorbent.

Fig. 4 Effect of pH on biosorption capacity of Cr(VI) at optimum dosage of RDSF, SDSF, and PDSF biosorbents



Effect of temperature

The effect of temperature (303 K to 333 K) was studied by changing the initial Cr(VI) concentration (100 mg/L to 300 mg/L), with 0.2 g/L of biosorbent dosage and maintained the solution pH at 2.

The mixture of biosorbent and Cr(VI) solution were kept in an orbital shaker at 100 rpm for 60 min. The results obtained are shown in Fig. 5 which denotes that the maximum biosorption capacity was observed at temperature 333 K for all the three (RDSF, SDSF, and PDSF) biosorbents. The maximum adsorption of Cr(VI) at higher temperature is attributed to the increase in mobility of chromium ions within the adsorbents' pore network. In addition, enhancement in the biosorption of Cr(VI) phenomenon at higher temperature can also be described by the creation of some new biosorption sites owing to the cracking of bond between molecules of the biosorbents (Singh et al. 2005).

Effect of adsorbent dose

The impact of biosorbent dosage (0.2 to 5 g/L) on Cr(VI) biosorption was investigated at room temperature while the other parameters such as agitation speed (100 rpm), contact time (60 min), pH (2), and hexavalent chromium concentration (100 mg/L) were kept constant. The results obtained are shown in Fig. 6 which confirm that the biosorption capacity decreases whereas the percentage elimination of Cr(VI) increases from 31.49 to 66.92%, 32.12 to 94.67%, and 30.28 to

84.67% for RDSF, SDSF, and PDSF biosorbents, respectively, with an increase in biosorbent dosage. The percentage elimination of Cr(VI) increases (refer to Fig. 6) from 31.49 to 66.92%, 32.12 to 94.67%, and 30.28 to 84.67% for RDSF, SDSF, and PDSF biosorbents respectively.

These results are attributed to the increased surface area as well as increased number of binding sites with increased in biosorbent dosage. However, the uptake of hexavalent chromium from solution is decreased from 69.73 to 29.46, 80.30 to 49.34, and 75.70 to 46.34 mg/g on RDSF, PDSF, and SDSF biosorbents respectively. This is likely due to the aggregation of biosorbent particles and unsaturated sites on biosorbent. Consequently, the active sites are deprived from being bind by metal ions (Albadarin et al. 2012; Khoubestani et al. 2015).

Impact of initial Cr(VI) ion concentration and interaction time

Both interaction time and initial Cr(VI) concentration are significant factors in determining the hexavalent Chromium elimination through biosorption process. The elimination of Cr(VI) from simulated solution was done with different initial concentrations (100 ppm 150 ppm 250 ppm and 300 ppm) of biosorbate and with various contact time (from 20 min to 140 min) at optimized condition i.e. biosorbents dosage (1 g/L), pH (2), 100 rpm agitation speed and at room temperature. The results obtained are shown in Fig. 7. As shown in this plot

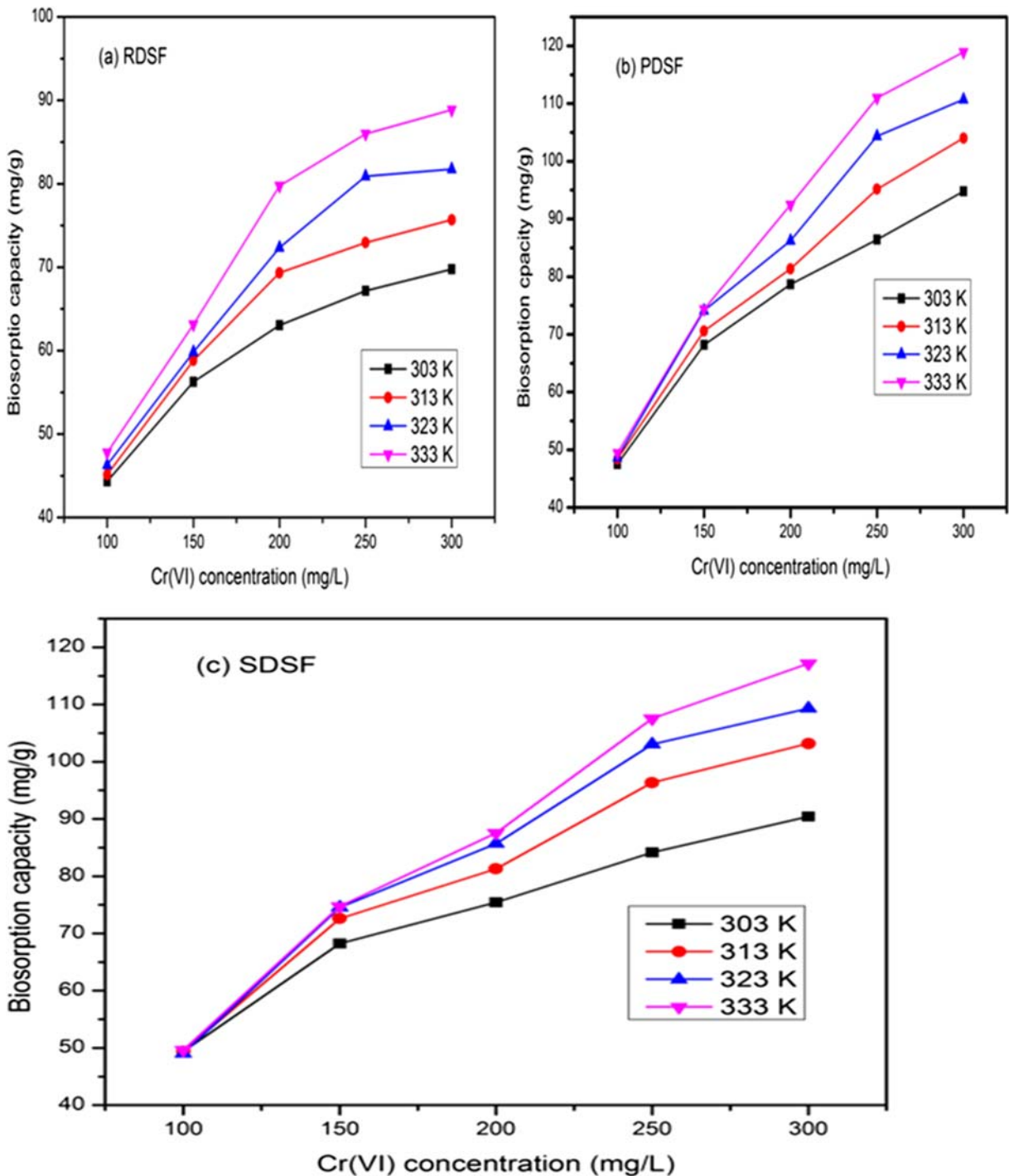
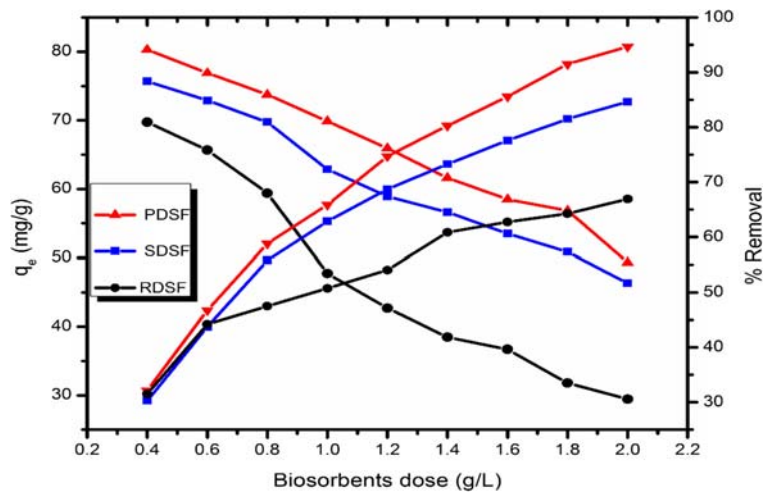


Fig. 5 Effect of temperature and initial Cr(VI) ion concentration on adsorption capacity of RDSF, SDSF, and PDSF biosorbents

the biosorption capacity increases steeply with an increase in initial concentration of Cr(VI). Eventually, the adsorption capacity attained the equilibrium

value with further increase in contact time. As the initial concentration increased from 100 to 300 ppm, the adsorption capacity is increased from 44.34 to

Fig. 6 Effect of biosorption capacity and the percentage Cr(VI) removal at 100 mg/L initial Cr(VI) concentration by different dosages of RDSF, SDSF, and PDSF biosorbents



69.76, 47.55 to 94.79, and 49.39 to 90.43 mg/g for RDSF, PDSF and SDSF respectively. This is likely due to the greater driving force (concentration gradient of Cr(VI) ions between the simulated solution of Cr(VI) and the adsorbent surface) at higher Cr(VI) concentrations. It is also attributed to more collisions between the adsorbate and adsorbent. At equilibrium, all the active sites are occupied by Cr(VI) ions (Singha and Das 2011).

Isotherm studies

Adsorption isotherms are used to examine the equilibrium characteristics of the biosorption phenomenon between the sorbate molecules adsorbed per unit mass of biosorbent. In the present investigation, various isotherm models such as Langmuir, Freundlich, and Dubinin–Radushkevich were selected to understand the biosorption process on the biosorbent’s surface. In each isotherm model, the initial metal ion concentration and the contact time was varied while the other parameters viz. biomass load, temperature, and pH were kept constant (Singha and Das 2011; Nasseh et al. 2017).

Langmuir isotherm model

In order to understand the adsorption phenomenon over homogeneous surface, Langmuir isotherm model was used, which postulates that there is no interaction among the sorbate molecules (Langmuir 1918). The Langmuir isotherm model equation in non-linear form is represented as follows:

$$q_e = \frac{q_m C_e b}{1 + bC_e} \tag{4}$$

The linear form of the model is expressed as follows:

$$\frac{C_e}{q_e} = \frac{1}{Q_0 b} + \frac{C_e}{Q_0} \tag{5}$$

Here, C_e represents the equilibrium Cr(VI) ion concentration (mg/L), b represents equilibrium constant (L/mg) which indicates the heat of sorption, Q_0 denotes maximum monolayer biosorption capacity, and q_e represents the amount of Cr(VI) biosorbed on unit mass biosorbent at equilibrium. The intercept and slope of plot C_e/q_e against C_e (refer to Fig. 8) were used to evaluate the values of b and Q_0 . The values of determination coefficient (R^2) and isotherm model are stated in Table 1. The calculated determination coefficient (R^2) data for all the three biosorbents (RDSF, PDS,F and SDSF) were close to 1 which indicated better agreement with Langmuir isotherm model. The significant characteristics parameters of Langmuir isotherm can be expressed in terms of separation factor, R_L . It is the dimensionless quantity, which is expressed by the following equation:

$$R_L = \frac{1}{1 + bC_i} \tag{6}$$

where C_i is the initial metal concentration and b represents the Langmuir constant. R_L values provide the information about the nature of adsorption process to be either unfavorable if $R_L > 1$, linear if $R_L = 1$, favorable if $0 < R_L < 1$, and irreversible if $R_L = 0$ (Dehghani et al. 2016; Gupta and Rastogi

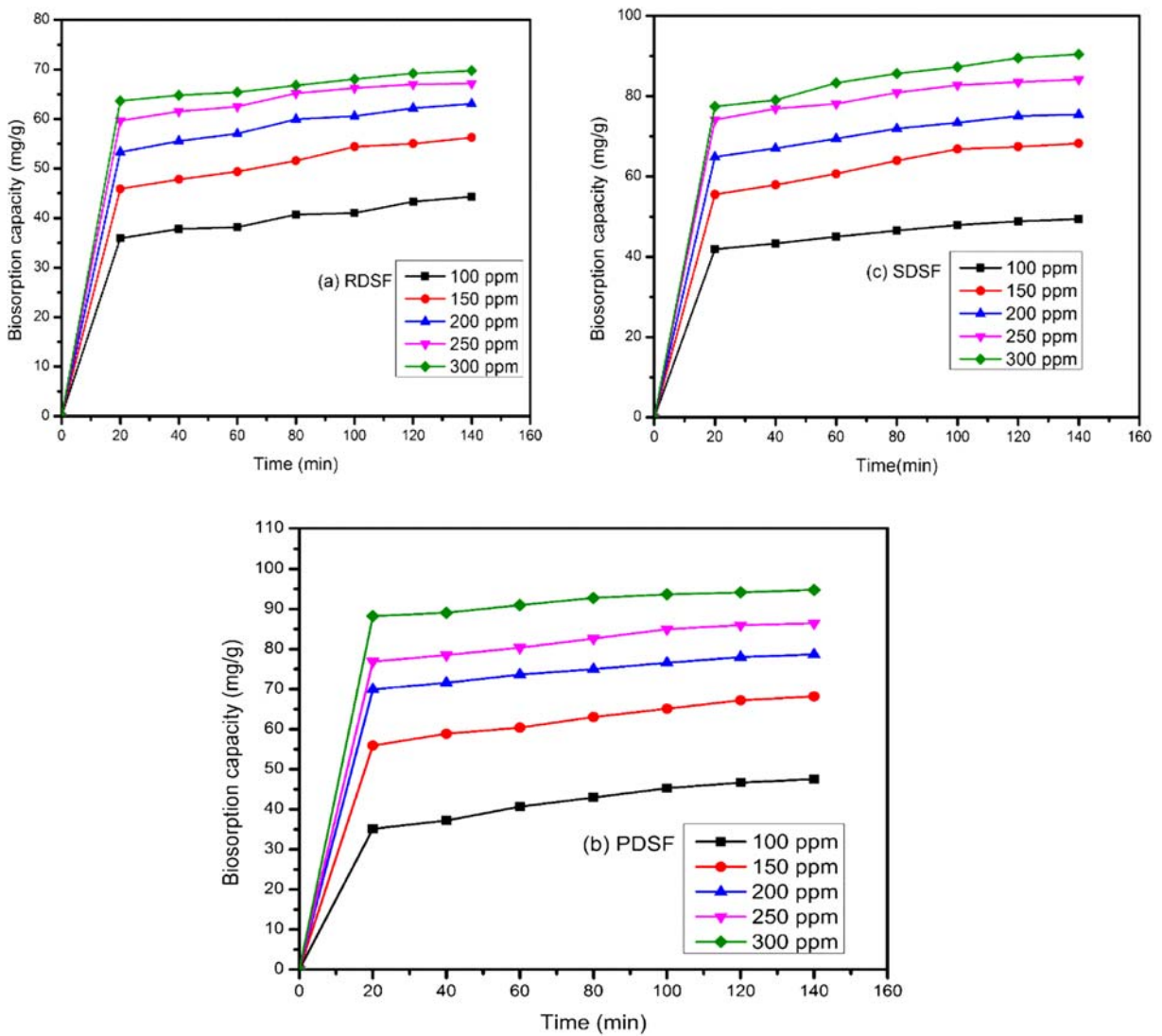


Fig. 7 Effect of contact time on biosorption capacity of Cr(VI) for RDSF, SDSF and PDSF biosorbents

2009; Sharma and Forster 1994). In the present study, it is clear from Table 1 that the observed R_L values are less than unity and more than 0 onto RDSF, SDSF, and PDSF biosorbents and validate that the Langmuir isotherm is favorable for adsorption.

Freundlich isotherm model

The Freundlich isotherm was employed to determine the multilayer sorption of the sorbate molecules over heterogeneous surfaces. The non-linear form of Freundlich equation is written form as follows:

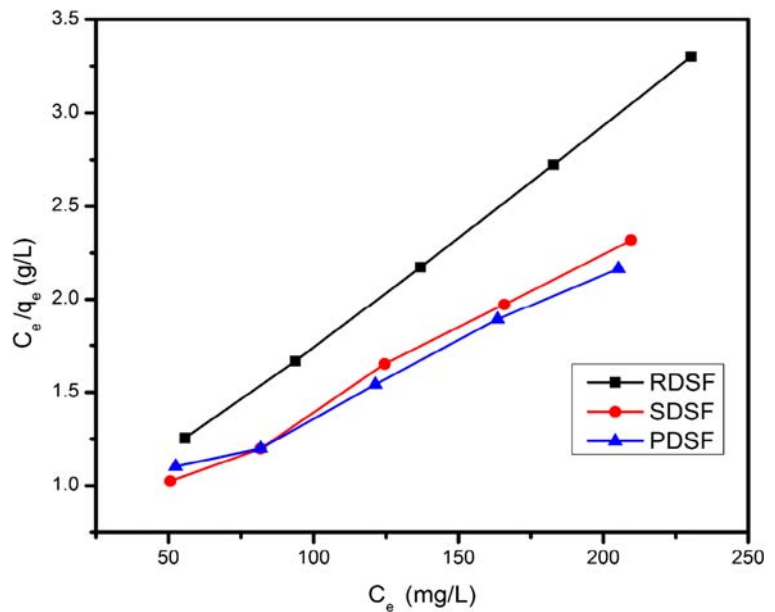
$$q_e = K_f C_e^{1/n_f} \tag{7}$$

The Freundlich model in logarithmic linear form is given by the following equation (Freundlich and Heller 1939):

$$\log q_e = \log K_f + \frac{1}{n_f} \log C_e \tag{8}$$

where K_f ($\text{mg}^{1-1/n_f} \text{L}^{1/n_f}/\text{g}$) and n_f represents the Freundlich isotherm biosorption capacity and biosorption intensity parameters respectively. The value of n_f greater than 1 indicates the higher

Fig. 8 Langmuir isotherm plots for Cr(VI) adsorption onto the RDSF, SDSF, and PDSF biosorbents



intensity of adsorption. The plot of $\log q_e$ versus C_e was used to evaluate n_f and K_f . In this study, the values of Freundlich constant parameter “ n_f ” was found to be as 3.137, 2.451, and 1.950 for RDSF, SDSF, and PDSF biosorbents respectively. Therefore, the values of “ n_f ” suggest that the biosorption process is favorable under the studied conditions.

Energy of sorption by Dubinin–Radushkevich model

The characteristics of the sorption curve which is associated with porosity of the adsorbent were studied by using Dubinin–Radushkevich (D-R) model (Dada et al. 2012).

Linearized equation of the D-R isotherm model can be denoted as:

Table 1 Biosorption isotherm constants obtained for various models obtained through linear regression analysis for Cr(VI) removal by RDSF, SDSF, and PDSF biosorbents

Isotherm model	Parameters	RDSF	SDSF	PDSF
Langmuir	Q_0 (mg/g)	84.745	119.05	135.0
	b (L/g)	0.020	0.014	0.011
	R^2	0.999	0.995	0.993
	R_L	0.329	0.406	0.471
Freundlich	K_f ($\text{mg}^{1-1/n} \text{L}^{1/n}/\text{g}$)	12.752	6.415	10.493
	n_f	3.137	2.451	1.950
	R^2	0.964	0.958	0.958
Dubinin–Radushkevich	Q_m (mg/g)	69.296	93.232	88.243
	K_{DR} (mol^2/J^2)	0.0002	0.0003	0.0002
	E (KJ/mol)	0.05	0.05	0.041
	R^2	0.971	0.977	0.964

$$\ln q_e = \ln Q_{m,DR} - K_{DR} \epsilon^2 \quad (9)$$

where $Q_{m, DR}$ denotes the observed biosorption capacity and K_{DR} denotes the biosorption energy (mol^2/J^2).

ϵ is the Polanyi potential and it is obtained by the following equation:

$$\epsilon = RT \ln \left(1 + \frac{1}{C_e} \right) \quad (10)$$

$Q_{m, DR}$ and K_{DR} constant can be obtained from the plot of $\ln q_e$ against ϵ^2 using the linear equation of D-R isotherm and the values are stated in Table 1.

The general form of energy release in the adsorption process (E , KJ/mol) is given as follows:

$$E = \frac{1}{\sqrt{2}K_{DR}} \quad (11)$$

Mean free energy (E) can be used to interpret the process of biosorption. If E ranges between 8 and 16 kJ/mol, then chemisorption process prevails and if $E < 8$ kJ/mol, then biosorption follows physisorption (Sari and Tuzen 2008; Lodeiro et al. 2006). The values of mean energy of Cr(VI) biosorption were calculated as 0.05, 0.05, and 0.041 kJ/mol on RDSF, SDSF, and PDSF biosorbents respectively. The mean free energy obtained for this study was less than 8 kJ/mol in all the three cases which suggested that the adsorption followed physisorption process. Determined R^2 values of Freundlich and Dubinin–Radushkevich (D-R) model for RDSF, SDSF, and PDSF biosorbents are less than those of Langmuir isotherm R^2 value as shown in Table 1. These results suggested that the D-R isotherm model was least agreeable with observed experimental values. Similar result was also reported in the literature (Khan et al. 2016; Yang and Chen 2008; Pandey et al. 2010).

Isotherm analysis by non-linear regression approach

The simulated data obtained for different adsorption isotherm models from non-linear regression analysis are shown in Fig. 9 and the best-fit isotherm parameters are presented in Table 2. It is clearly evident that χ^2 value is minimum for Langmuir adsorption isotherm. Thus, both linear (high R^2 value) and non-linear (low χ^2

value) regression analysis suggest that Langmuir isotherm model could explain the adsorption process better in comparison to other isotherm models. Similar finding is reported in other literature as well (Apiratikul and Pavasant 2008).

Adsorption thermodynamics

The thermodynamic studies were performed to understand the feasibility and thermal effect on biosorption process onto the surfaces of RDSF, SDSF, and PDSF. Van't Hoff and Gibb's Helmholtz equations were used to analyze the thermodynamic process of biosorption (Pandey et al. 2010).

$$\Delta G^0 = RT \ln K_C \quad (12)$$

$$K_C = \frac{C_a}{C_e} \quad (13)$$

$$\ln K_C = \frac{\Delta H^0}{RT} + \frac{\Delta S^0}{R} \quad (14)$$

where K_C represents the equilibrium constant; C_a and C_e represent the concentration of Cr(VI) at solid phase and in aqueous phase at saturation stage, respectively; R represents the universal gas constant; and temperature is represented as T (in Kelvin). Calculated values of ΔG^0 , ΔS^0 , and ΔH^0 for the current study are represented in Table 3. Negative values of ΔG^0 indicated that biosorption process was spontaneous and favorable with the increase in temperature. The possible reason could be the faster diffusion of Cr(VI) ions from bulk solution phase to biosorbent at higher temperatures. ΔH^0 and ΔS^0 values (refer Table 3) were observed from the values of slope and intercept of $\ln K_C$ vs $1/T$ plot and it suggested that biosorption was endothermic and highly arbitrary in nature at the liquid–solid interface (Hasan et al. 2008; Rangabhashiyam and Selvaraju 2015a, 2015b).

Determination of activation energy

The temperature dependence activation energy of adsorption was determined by the linear form of Arrhenius equation and it is expressed by the following equation (Argun and Dursun 2008).

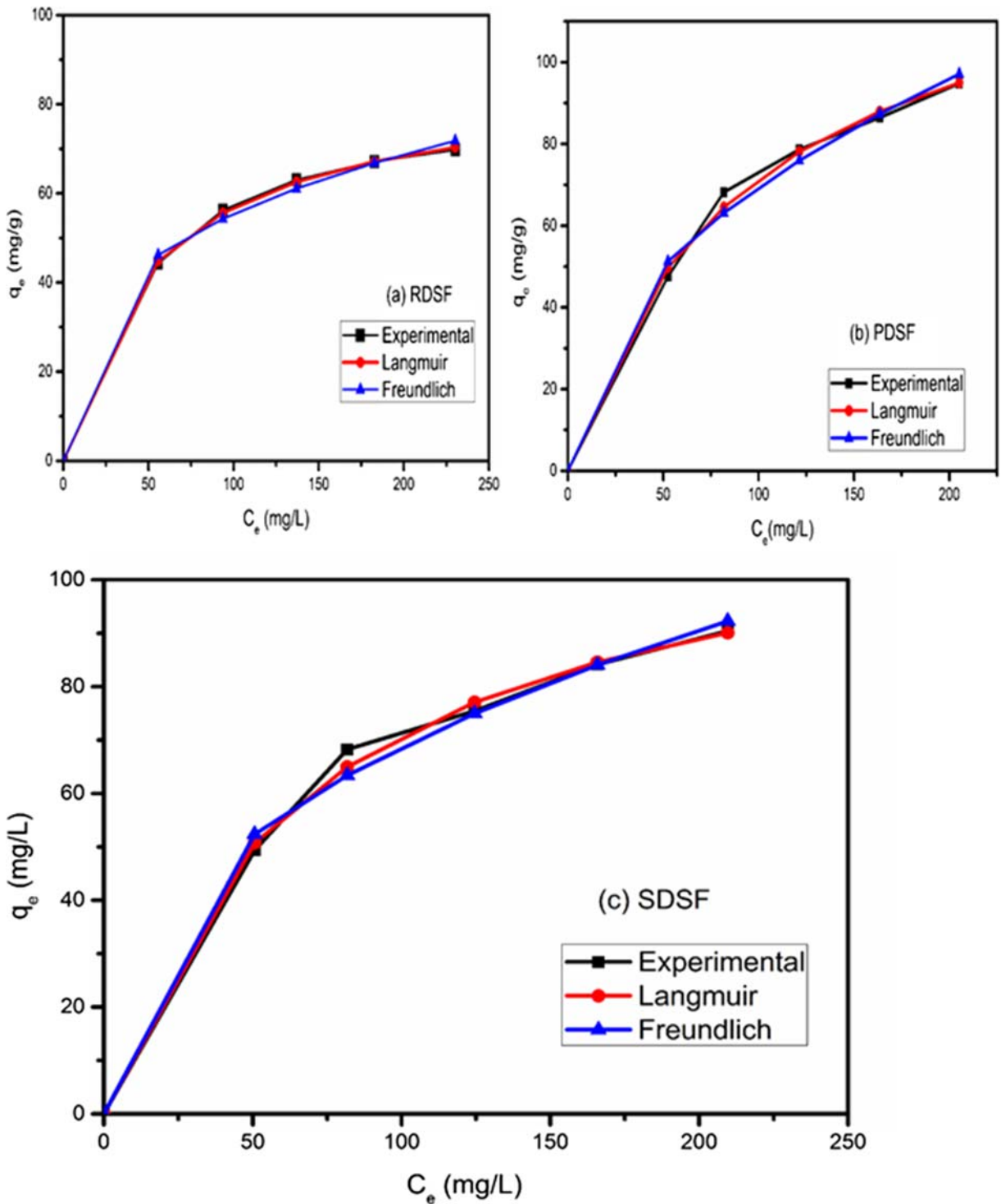


Fig. 9 Isotherm model curves fitted by non-linear regression analysis for Cr(VI) biosorption on RDSF, SDSF, and PDSF biosorbents

Table 2 Langmuir and Freundlich isotherm parameters along with chi-square value as observed by the error analysis method

Isotherm model	Parameters	RDSF	SDSF	PDSF
Langmuir	Q_0 (mg/g)	85.916	119.632	138.074
	b (L/g)	0.020	0.015	0.011
	χ^2	0.020	0.231	0.326
Freundlich	K_f ($\text{mg}^{1-1/n} \text{L}^{1/n}/\text{g}$)	13.245	10.954	8.029
	$1/n_f$	0.311	0.399	0.468
	χ^2	0.266	0.564	0.828

$$\ln K_2 = \ln A - \frac{E_a}{RT} \tag{15}$$

where K_2 denotes the rate constant of pseudo-second-order model (g/mg min), A indicates the Arrhenius factor, E_a represents the activation energy, T represents the solution temperature (K), and R is a gas constant (8.314 J/mol K). The activation energy provides information about the type of adsorption process, i.e.,

whether it is chemical or physical (Argun et al., 2008, Mahmoud 2015). It is also reported that the physisorption process normally requires less energy (0–40 kJ/mol) comparing to chemisorption (40–800 kJ/mol) since the force involved between adsorbate and adsorbent is weak and the process rapidly attained the equilibrium. The activation energy is estimated from the slope of $\ln K_2$ vs $1/T$ plot (figure not shown). The calculated activation energy values for sorption are

Table 3 Thermodynamic parameters for biosorption of Cr (VI) onto the raw and chemically modified *Datura stramonium* fruit biosorbents

Initial Cr concentration (mg/L)	Temp. (K)	RDSF				PDSF				SDSF			
		K_c	ΔG° (kJ/mol)	ΔH° (kJ/mol)	ΔS° (kJ/Kmol)	K_c	ΔG° (kJ/mol)	ΔH° (kJ/mol)	ΔS° (kJ/Kmol)	K_c	ΔG° (kJ/mol)	ΔH° (kJ/mol)	ΔS° (kJ/Kmol)
100 ppm	303	0.796	-0.249	1.680	0.004	0.975	-0.026	0.037	0.002	0.906	-0.107	0.864	0.031
	313	0.822	-0.220			0.976	-0.026			0.937	-0.073		
	323	0.862	-0.172			0.961	-0.045			0.947	-0.062		
	333	0.915	-0.106			0.984	-0.018			0.977	-0.027		
150 ppm	303	0.600	-0.558	2.194	0.005	0.834	-0.197	2.104	0.006	0.833	-0.198	2.155	0.006
	313	0.645	-0.495			0.938	-0.072			0.889	-0.133		
	323	0.663	-0.477			0.987	-0.014			0.977	-0.027		
	333	0.727	-0.383			0.992	-0.009			0.983	-0.020		
200 ppm	303	0.460	-0.848	4.229	0.011	0.605	-0.548	5.728	0.017	0.648	-0.474	3.437	0.009
	313	0.530	-0.716			0.684	-0.427			0.685	-0.426		
	323	0.567	-0.661			0.822	-0.336			0.758	-0.323		
	333	0.663	-0.493			0.963	-0.300			0.860	-0.181		
250 ppm	303	0.367	-1.095	4.435	0.011	0.507	-0.742	4.785	0.013	0.528	-0.697	5.070	0.014
	313	0.412	-1.002			0.627	-0.527			0.614	-0.549		
	323	0.478	-0.860			0.701	-0.413			0.716	-0.388		
	333	0.524	-0.776			0.755	-0.337			0.798	-0.270		
300 ppm	303	0.303	-1.306	3.967	0.008	0.431	-0.919	4.714	0.012	0.462	-0.844	4.207	0.011
	313	0.337	-1.227			0.524	-0.729			0.530	-0.715		
	323	0.374	-1.145			0.580	-0.633			0.585	-0.625		
	333	0.420	-1.040			0.640	-0.535			0.657	-0.505		

found to be 0.192, 7.632, and 7.794 kJ/mol for RDSF, SDSF, and PDSF respectively which confirm that adsorption on the studied biosorbent is physical in nature. In addition, it is evident from Table 1 that the mean free energy estimated by using Dubinin–Radushkevich model is also less than 8 kJ/mol which confirms that the adsorption is physical in nature (Gupta et al. 2010).

Adsorption kinetics

The mechanism and the rate-controlling steps of adsorption process over a series of contact time for different initial Cr(VI) concentrations was studied by adsorption kinetic models. Various kinetics models (pseudo-first-order, intraparticle diffusion model, and pseudo-second-order kinetics models) were selected to study the adsorption mechanism and the fittings of these model are shown in Fig. 10.

Pseudo-first-order kinetics

Lagergren proposed the pseudo-first-order model assuming that the rate of change in concentration of the reactants with time is directly proportional to gradient of solute in solution. The general form of the equation can be stated as follows (Lagergren 1898):

$$\frac{dq_t}{dt} = k_1(q_e - q_t) \tag{16}$$

The equation in non-linear model can be expressed as follows:

$$q_t = q_e - q_e \exp(-K_1 t) \tag{17}$$

The linear form of pseudo-first-order equation can be written as follows:

$$\log(q_e - q_t) = \log q_{e \text{ cal}} - \frac{k_1}{2.030} t \tag{18}$$

where q_e and q_t denote the uptake capacity of Cr(VI) at equilibrium and at given time “ t ” respectively (Hasan et al. 2008). The values of equilibrium metal concentration $q_{e \text{ (cal)}}$, rate constant k_1 , and coefficient of determination (R^2) can be obtained by plotting $\log(q_e - q_t)$ against t . R^2 values of pseudo-first-order are presented in Table 4 which infer poor correlation coefficient for Cr(VI) adsorption. From Table 4, it can be indicated

that calculated $q_{e(\text{cal})}$ values were least fit with the experimental q_e values compared to other kinetic models.

Pseudo-second-order kinetics

This model was proposed to study the chemical sorption mechanism by Ho and McKay (Ho and McKay 1999). The equation can be represented in non-linear form as follows:

$$q_t = \frac{tK_2q_e^2}{1 + tK_2q_e} \tag{19}$$

The simple form of pseudo-second-order model can be expressed as:

$$\frac{t}{q_t} = \frac{1}{k_2q_e^2} + \frac{t}{q_e} \tag{20}$$

The observed pseudo-second-order rate constant k_2 (g/mg/min), the correlation coefficient R^2 , and the calculated biosorption capacity at time t and at equilibrium, i.e., q_t and q_e respectively are listed in Table 4. The plot of t/q_t vs t are shown in Fig. 11 for the biosorption of Cr(VI) species onto the surface of RDSF, SDSF, and PDSF.

Table 4 suggests that the R^2 values of pseudo-first-order is fitting poorly to the experimental data than the pseudo-second-order kinetics (closer to 1). Moreover, the predicated values of biosorption capacity at equilibrium mimic the experimental values. Therefore, it can be concluded that biosorption of Cr(VI) onto RDSF, SDSF, and PDSF is explained better by pseudo-second-order kinetics and chemisorption may be the rate controlling step in biosorption which possibly occurred via electron exchange (Gonzalez et al. 2008).

Intraparticle diffusion model

To understand the mass transfer mechanism onto the surface of RDSF, SDSF, and PDSF, intraparticle diffusion model was used. It was proposed by Weber and Morris and the general form of equation can be stated as (Weber and Morris 1963; Hasan et al. 2008):

$$q_t = k_{id}t^{1/2} + c \tag{21}$$

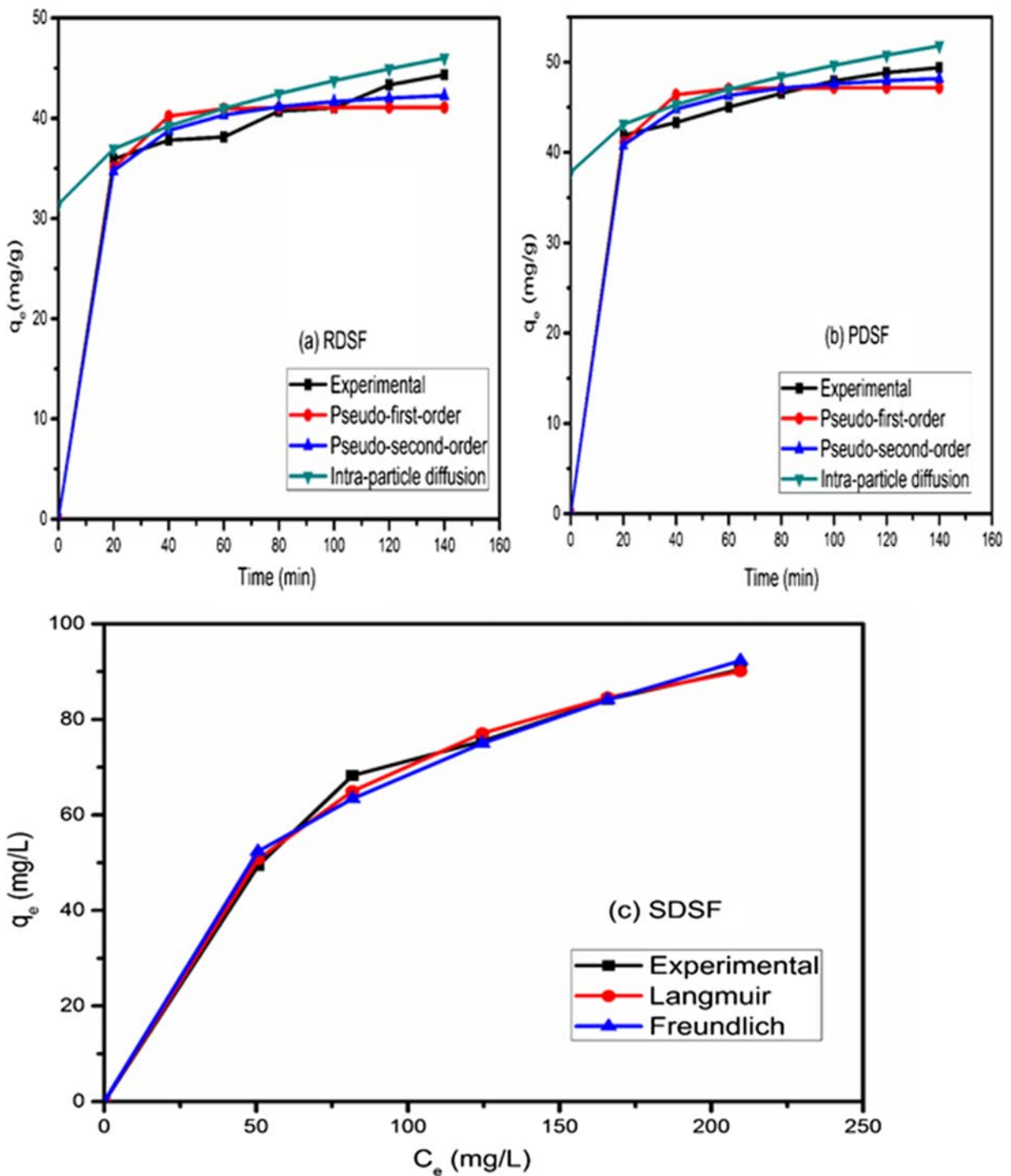


Fig. 10 Kinetics model curves fitted by non-linear approach for Cr(VI) biosorption onto RDSF, SDSF, and PDSF biosorbents

where K_{id} ($\text{mg/g min}^{1/2}$) represents the rate constant for intraparticle diffusion, q_t is the capacity of solute biosorbed on biosorbents, and C (mg/g) gives the

information about boundary layer. The plot q_t against $t^{1/2}$ was used to observe the data of K_{id} and C , which are represented in Table 4. It can be

Table 4 Estimated kinetic parameters for biosorption of Cr(VI) onto the raw and chemically modified *Datura stramonium* fruit surface

Sample	Cr(VI) conc. (mg/L)	q_e (exp) (mg/g)	Pseudo first order			Pseudo second order			Intraparticle diffusion		
			k_1 (min^{-1})	q_e (cal) (mg/g)	R^2	k_2 (g/mg/min)	q_e (cal) (mg/g)	R^2	k_{id} (mg/g/min ^{1/2})	C (mg/g)	R^2
RDSF	100	44.34	0.019	15.24	0.902	0.002	46.3	0.995	1.143	30.34	0.956
	150	56.26	0.022	13.53	0.93	0.002	59.17	0.997	1.492	38.63	0.978
	200	63.04	0.023	18.81	0.931	0.002	65.36	0.998	1.37	47.03	0.987
	250	67.16	0.035	24.22	0.896	0.003	69.44	0.999	1.116	54.56	0.968
	300	69.76	0.022	12.62	0.867	0.004	71.43	0.999	0.869	59.32	0.972
PDSF	100	49.39	0.025	16.33	0.931	0.003	51.28	0.998	1.081	36.83	0.992
	150	68.24	0.028	31.2	0.939	0.002	71.94	0.998	1.889	46.68	0.977
	200	75.44	0.03	27.93	0.883	0.002	78.13	0.999	1.542	57.74	0.99
	250	84.15	0.028	22.8	0.942	0.002	89.29	0.994	1.794	65.75	0.818
	300	90.43	0.025	28.48	0.912	0.002	94.34	0.999	0.114	75.54	0.97
SDSF	100	47.55	0.026	27.68	0.937	0.001	51.55	0.996	1.08	26.44	0.988
	150	68.2	0.023	25.36	0.893	0.002	71.43	0.997	1.721	47.87	0.991
	200	78.66	0.024	18.61	0.901	0.003	80.65	0.999	1.243	64.07	0.994
	250	86.45	0.029	25.83	0.895	0.002	92.59	0.99	1.95	67.06	0.714
	300	94.79	0.024	13.71	0.968	0.004	96.15	0.999	0.951	83.71	0.949

inferred from the results that the value of C increases as initial concentration of Cr(VI) ion increases. It is likely due to the increase in boundary layer thickness. The dual nature of the plot (Fig. 12) was credited to the adsorption phenomenon. If the plot q_t against $t^{1/2}$ passes via origin, then it indicates that intraparticle diffusion process is the rate regulatory step in biosorption process; otherwise, it implies that some other mechanism also will be involved. In fact, the plot obtained is multilinear, indicating that biosorption of Cr(VI) is affected by more than one process. The first stage of graph suggested that an external mass transfer to the surface of absorbent from liquid solution is the rate-determining step, whereas the second stage indicated pore diffusion or intraparticle diffusion is the rate controlling mechanism.

Kinetic model analysis by non-linear regression analysis

Kinetic parameters were also evaluated by non-linear regression analysis. The determined kinetic parameters values are summarized in Table 5.

From Tables 4 and 5, it can be revealed that the values of R^2 and χ^2 of pseudo-second-order model are higher and lower respectively than the other kinetic models used in this study. In addition, the theoretical q_e values evaluated by pseudo-second-order are closer to experimental values. Hence, both these observations implied that the adsorption of Cr(VI) on biosorbent is better described by pseudo-second-order model. These findings also suggested that the chemisorption process may be the rate-limiting step and similar conclusions were observed by other researchers also (Bansal et al. 2009; Muthukumaran and Beulah 2011).

Desorption

Desorption studies reveal information about biosorbent’s potential to be regenerated and reused for commercial scale application. One molar of HCl was used for the desorption of Cr(VI) from biosorbents. For this study, three consecutive adsorption–desorption cycles were performed. Protons (H^+) ions from HCl solution displaces the chelated Cr(VI) metal ion from the biosorbent’s

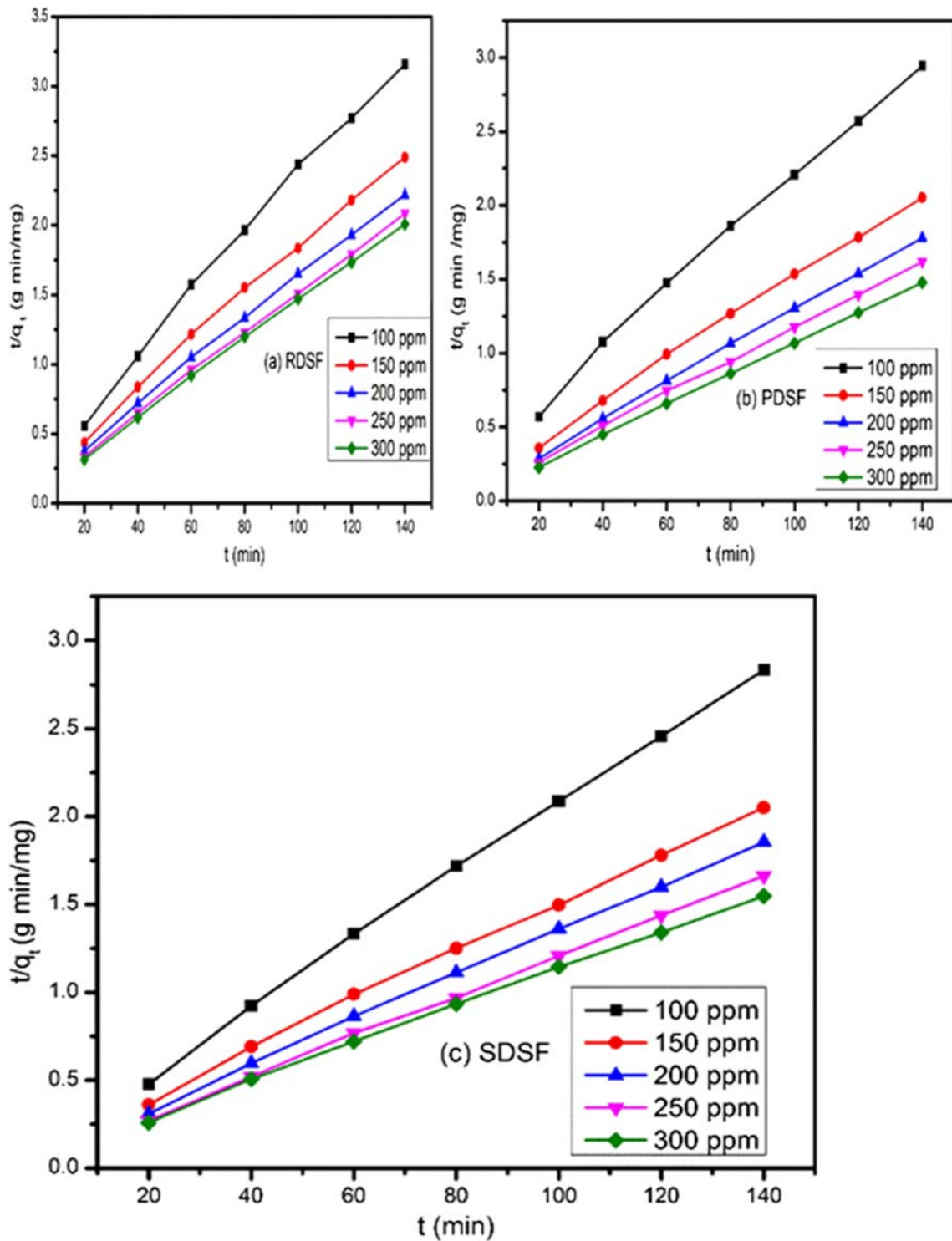


Fig. 11 Pseudo-second-order plots for adsorption of Cr(VI) onto the RDSF, SDSF, and PDSF biosorbents

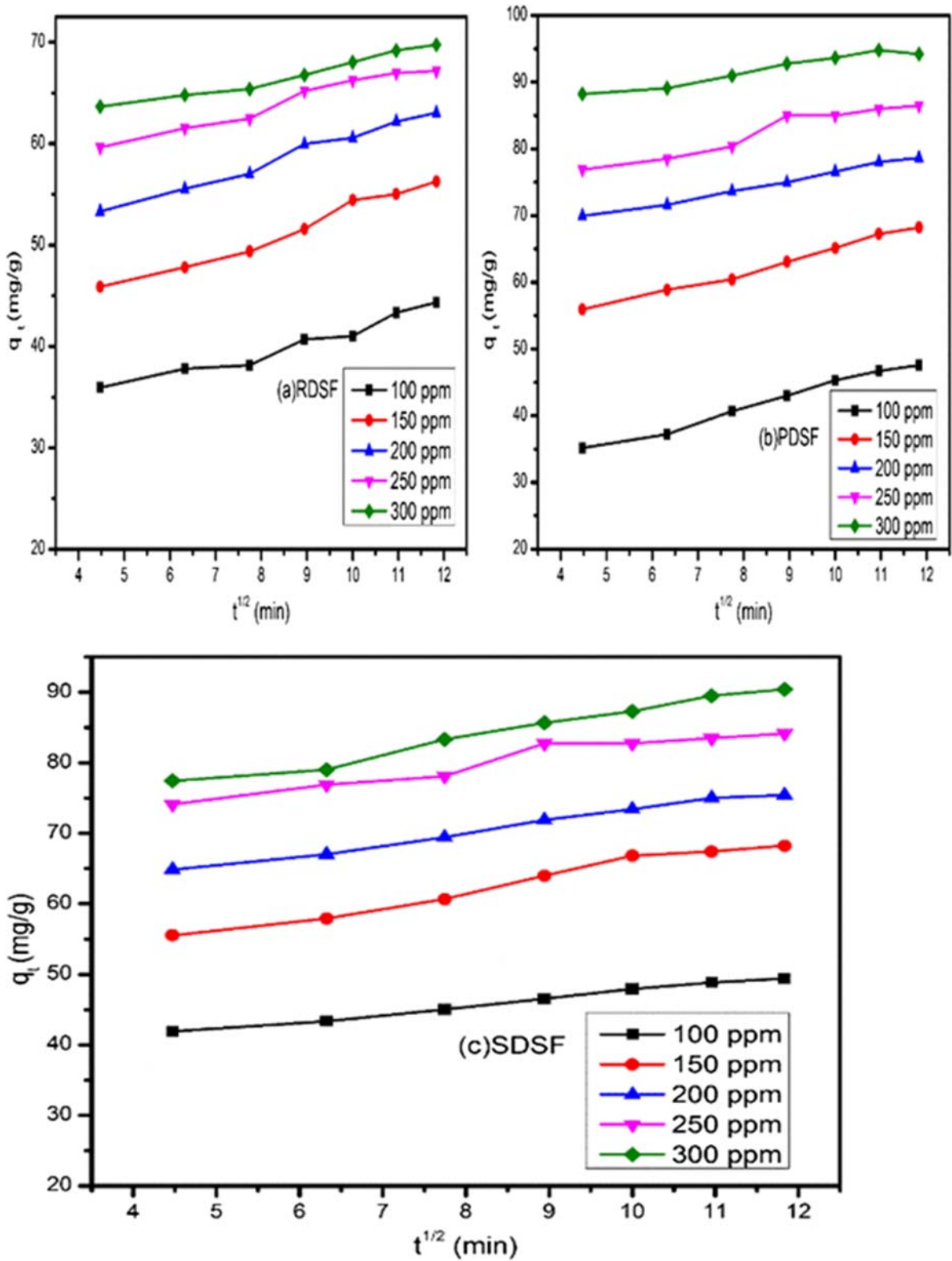


Fig. 12 Intraparticle diffusion model plots for the biosorption of Cr(VI) by RDSF, PDSF, and SDSF biosorbents

Table 5 Kinetic parameters determination using non-linear regression analysis

Sample	Cr(VI) Conc. (mg/L)	q_e (exp) (mg/g)	Pseudo first order			Pseudo second order			Intraparticle diffusion		
			k_1 (min^{-1})	q_e (cal) (mg/g)	χ^2	k_2 (g/mg/min)	q_e (cal) (mg/g)	χ^2	k_{id} (mg/g/min ^{1/2})	C (mg/g)	χ^2
RDSF	100	44.34	0.096	41.08	0.738	0.004	43.833	0.340	1.143	30.34	0.667
PDSF		49.39	0.103	47.15	0.490	0.005	49.67	0.172	1.180	37.84	0.516
SDSF		47.55	0.067	44.31	1.208	0.002	49.01	0.440	1.888	27.64	0.511

surface during regeneration process. The regeneration results revealed (shown in Fig. 13) a percentage reduction in adsorption capacity for each step of regeneration cycle such as the following: from 71.12% (1st cycle), 62.45% (2nd cycle), to 42.34% (3rd cycle) for PDSF; from 64.43% (1st cycle), 51.01% (2nd cycle), to 29.87% (3rd cycle) for SDSF; and from 52.54% (1st cycle), 34.70% (2nd cycle), to 12.09% (3rd cycle) for RDSF biosorbents. This is likely due to the structural changes of biosorbents' surface with the binding of Cr(VI) ions (Muthukumaran and Beulah 2011; Pourfadakari et al. 2017).

Economic study of the adsorbent

According to the results obtained in the present study, 1 m³ of Cr(VI)-containing wastewater could be treated by using 1.1-kg biosorbent derived from

Datura stramonium fruit. The sorbent derived from *Datura stramonium* used in the present study has no cost associated with it. However, cost estimation for processing and transporting the biosorbent has been carried out by considering 1 kg of biosorbents and the cost involved in each step of preparation process is summarized in Table 6. Generally, the cost of the activated carbon utilized as an adsorbent for removing toxic metal from wastewater is approximately \$2000 USD/ton in India (Rangabhashiyam and Selvaraju 2015a, 2015b). Considering the account of expense, it is clear from Table 6 that the cost of derived biosorbent from *Datura stramonium* is very low and reasonable (\$124.51, \$517.76, and \$1079.01 USD/ton for RDSF, SDSF, and PDSF biosorbents respectively) compared to conventionally activated carbon. Hence, it can be inferred that the derived biosorbent from *Datura stramonium* fruit may be

Fig. 13 Desorption of Cr(VI)-loaded biosorbents for the reutilization process of Cr(VI) ions

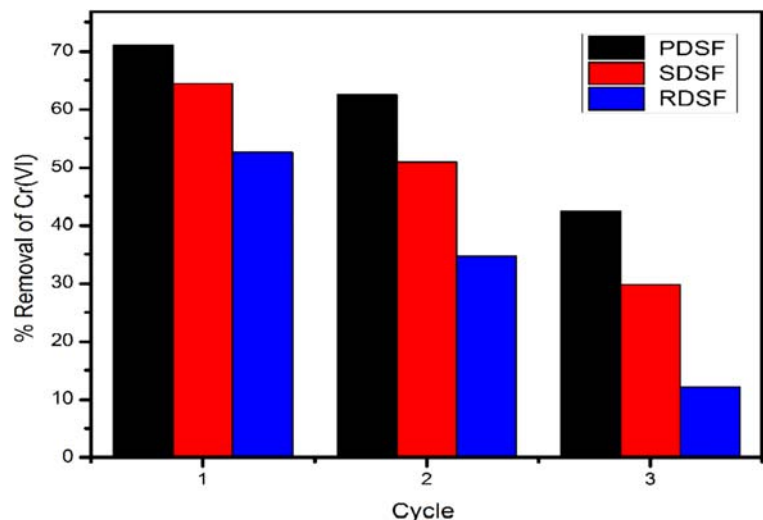


Table 6 Cost estimation for the biosorbent derived from *Datura stramonium* fruit

Sr. no.	Material used	Unit cost (Rs.)	RDSF		SDSF		PDSF	
			Amount used	Net price (Rs.)	Amount used	Net price (Rs.)	Amount used	Net price (Rs.)
1	Transportation	4		4	–	–	–	–
2	Sulfuric acid	10/kg	0	0	1 kg	10	–	–
3	Phosphoric acid	50/kg	0	0	–	–	1 kg	50
4	NaHCO ₃	0.554/L	0	0	5 L	2.77	5 L	2.77
5	Cost of drying-1	5/kWh	0.83 kWh (80 °C for 24 h)	4.15	0.83 kWh (105 °C for 24 h)	4.15	0.83 kWh (110 °C for 24 h)	4.15
6	Cost of heating-1	5/kWh	–	–	4 kWh (105 °C for 24 h)	20	–	–
7	Cost of heating-2	5/kWh	–	–	–	–	4 kWh (105 °C for 24 h)	20
8	Net cost (Rs.)	–	–	8.96	–	36.91	–	76.92
9	Other charges (1% of net cost)	–	–	0.815	–	0.3691	–	0.7692
10	Total cost (Rs./kg)	–	–	8.96	–	37.27	–	77.68
11	Total cost (US\$/ton)	–	–	124.51	–	517.76	–	1079.01

Table 7 Comparison of adsorption capacity of biosorbents

Biosorbent	Solution pH	Biosorption capacity (mg/g)	References
Chemically modified <i>Swietenia mahagoni</i> Shells (SSMS, PSMS, RSMS)	pH 2	47.61, 58.82, and 37.03	(Rangabhashiyam et al. 2015)
Coconut coir	pH 2	26.8	(Gonzalez et al. 2008)
Rice husk carbon (RHC) and saw dust carbon (SDC)	pH 2	48.31 and 53.48	(Bansal et al. 2009)
Chemically <i>Syzygium jambolanum</i> nut	pH 2	39.81	(Muthukumaran and Beulah 2011)
CAC-S, OS-S	pH 1.5	71.4 and 25.6	(Attia et al. 2010)
Neem sawdust	pH 2	58.82	(Vinodhini & Das 2010)
<i>Melaleuca diosmifolia</i> leaf	pH 2	62.5	(Kuppusamy et al. 2016)
Tobacco-leaf	pH 1	113.2	(Chen et al. 2009)
Mangrove leaf powder	pH 2.0	60.24	(Sathish et al. 2015)
Boiled sunflower head	pH 2	7.9	(Jain et al. 2009)
Peanut shell (P. Shell), sawdust and <i>Cassia fistula</i> leaves	pH 2	4.32, 3.66 and 4.48	(Ahmad et al. 2017)
Humane hair	pH 2	9.85	(Mondal and Basu 2019)
Cranberry (<i>Cornus mas</i>) kernel shell (CKS), rosehip (<i>Rosa canina</i>), seed shell (RSS), and banana (<i>Musa cavendishii</i>) peel (BP)	pH 2	10.42, 15.17, and 6.81	(Parlayici and Pehlivan 2019)
Acid activated banana peel (AABP) and organo-montmorillonite	pH 4	15.1 and 6.67	(Ashraf et al. 2017)
Raw and activated chestnut shells	pH 2	4.44 and 33	(Niazi et al. 2018)
RDSF	pH 2	85.91	Present study
SDSF	pH 2	119.63	Present study
PDSF	pH 2	138.07	Present study

employed as an alternatively inexpensive potential biosorbent for removing Cr(VI) from wastewater.

Comparison with other adsorbents

Comparison of biosorption capacities of PDSF, SDSF, and RDSF with earlier reported biosorbents are shown in Table 7. It is observed that biosorption capacity of the prepared biosorbents is higher than the other reported biosorbents for removal of Cr(VI). The adsorption capacity is attributed to several important factor such as the extent of surface modification and physical characteristics of biosorbents.

Conclusions

The present investigation is focused on potential of chemically modified and untreated biosorbent as low-cost biosorbent for removal of Cr(VI) from wastewater. The chemical and physical characteristics of biosorbent were observed by various technique like FTIR, SEM, and EDX. The equilibrium data is well explained by Langmuir isotherm model with high R^2 and low χ^2 value. The maximum monolayer biosorption capacity of Cr(VI) is 85.916, 119.632, and 138.074 mg/g on RDSF, SDSF, and PDSF respectively at optimum pH 2.0. The kinetics analysis revealed that biosorption is better followed by pseudo-second-order model with high R^2 and low χ^2 value. Among all the studied biosorbents, PDSF showed the maximum adsorption capacity ($Q = 138.074$ mg/g). The estimated activation energy and mean free energy (by Dubinin–Radushkevich model) suggested that adsorption process is mainly governed by physisorption mechanism. Thermodynamic investigation indicated the feasibility, spontaneous, and endothermic nature of adsorption. The present studies showed that PDSF offers an economical and efficient alternative biosorbent for Cr(VI) biosorption from wastewater.

References

- Abdel-Ghani, N. T., Hefny, M. M., & El-Chaghaby, G. A. (2008). Removal of metal ions from synthetic wastewater by adsorption onto eucalyptus camaldulensis tree leaves. *Journal of the Chilean Chemical Society*, 53, 1585–1587.
- Ahluwalia, S. S., & Goyal, D. (2005). Removal of heavy metals by waste tea leaves from aqueous solution. *Engineering in Life Sciences*, 5, 158–162.
- Ahmad, A., Ghazi, Z. A., Saeed, M., Ilyas, M., Ahmad, R., Khattak, A. M., & Iqbal, A. (2017). A comparative study of the removal of Cr(VI) from synthetic solution using natural biosorbents. *New Journal of Chemistry*, 41, 10799–10807.
- Albadarin, A. B., Mangwandi, C., Al-Muhtaseb, A. H., Walker, G. M., Allen, S. J., & Ahmad, M. N. M. (2012). Kinetic and thermodynamics of chromium ions adsorption onto low-cost dolomite adsorbent. *Chemical Engineering Journal*, 179, 193–202.
- Apiratikul, R., & Pavasant, P. (2008). Batch and column studies of biosorption of heavy metals by *Caulerpa lentillifera*. *Bioresource Technology*, 99, 2766–2777.
- Argun, M. E., & Dursun, S. (2008). A new approach to modification of natural adsorbent for heavy metal adsorption. *Bioresource Technology*, 99, 2516–2527.
- Ashraf, A., Bibi, I., Niazi, N. K., Ok, Y. S., Murtaza, G., Shahid, M., Kunhikrishnan, A., Li, D., & Mahmood, T. (2017). Chromium(VI) sorption efficiency of acid-activated banana peel over organo-montmorillonite in aqueous solutions. *International Journal of Phytoremediation*, 19, 605–613.
- Attia, A. A., Khedr, S. A., & Elkholy, S. A. (2010). Adsorption of chromium ion (VI) by acid activated carbon. *Brazilian Journal of Chemical Engineering*, 27, 183–193.
- Bansal, M., Singh, D., & Garg, V. K. (2009). A comparative study for the removal of hexavalent chromium from aqueous solution by agriculture wastes' carbons. *Journal of Hazardous Materials*, 171, 83–92.
- Barakat, M. A. (2011). New trends in removing heavy metals from industrial wastewater. *Arabian Journal of Chemistry*, 4, 361–377.
- Bellu, S., García, S., González, J. C., Atria, A. M., Sala, L. F., & Signorella, S. (2008). Removal of chromium(VI) and chromium(III) from aqueous solution by grainless stalk of corn. *Separation Science and Technology*, 43, 3200–3220.
- Blazquez, G., Hernáinz, F., Calero, M., Martín-Lara, M. A., & Tenorio, G. (2009). The effect of pH on the biosorption of Cr (III) and Cr (VI) with olive stone. *Chemical Engineering Journal*, 148, 473–479.
- Chen, Z., Ma, W., & Han, M. (2008). Biosorption of nickel and copper onto treated alga (*Undaria pinnatifida*): application of isotherm and kinetic models. *Journal of Hazard Materials*, 155, 327–333.
- Chen, Y., Tang, G., Yu, Q. J., Zhang, T., Chen, Y., & Gu, T. (2009). Biosorption properties of hexavalent chromium on tobacco-leaf residues. *Environmental Technology*, 30, 1003–1010.
- Dada, A. O., Olalekan, A. P., Olatunya, A. M., & Dada, O. (2012). Langmuir, Freundlich, Temkin and Dubinin–Radushkevich isotherms studies of equilibrium sorption of Zn^{2+} onto phosphoric acid modified rice husk. *IOSR Journal of Applied Chemistry*, 3(1), 38–45.
- Dehghani, M. H., Sanaei, D., Ali, I., & Bhatnagar, A. (2016). Removal of chromium (VI) from aqueous solution using treated waste newspaper as a low-cost adsorbent: Kinetic modeling and isotherm studies. *Journal of Molecular Liquids*, 215, 671–679.
- Etim, U. J., Umoren, S. A., & Eduok, U. M. (2016). Coconut coir dust as a low cost adsorbent for the removal of cationic dye

- from aqueous solution. *Journal of Saudi Chemical Society*, 20, S67–S76.
- Freundlich, H., & Heller, W. (1939). The adsorption of cis- and trans-Azobenzene. *Journal of the American Chemical Society*, 61, 2228–2230.
- Gonzalez, M. H., Araújo, G. C. L., Pelizaro, C. B., Menezes, E. A., Lemos, S. G., de Sousa, G. B., & Nogueira, A. R. A. (2008). Coconut coir as biosorbent for Cr(VI) removal from laboratory wastewater. *Journal of Hazardous Materials*, 159, 252–256.
- Gupta, V. K., & Rastogi, A. (2009). Biosorption of hexavalent chromium by raw and acid-treated green alga *Oedogonium hatei* from aqueous solutions. *Journal of Hazardous Materials*, 163, 396–402.
- Gupta, V. K., Rastogi, A., & Nayak, A. (2010). Adsorption studies on the removal of hexavalent chromium from aqueous solution using a low cost fertilizer industry waste material. *Journal of Colloid and Interface Science*, 342, 135–141.
- Hasan, S. H., Singh, K. K., Prakash, O., Talat, M., & Ho, Y. S. (2008). Removal of Cr(VI) from aqueous solutions using agricultural waste 'maize bran. *Journal of Hazardous Materials*, 152, 356–365.
- Ho Lee, S., Hun Jung, C., Chung, H., Yeal Lee, M., & Yang, J.-W. (1998). Removal of heavy metals from aqueous solution by apple residues. *Process Biochemistry*, 33, 205–211.
- Ho, Y. S., & McKay, G. (1999). Pseudo-second order model for sorption processes. *Process Biochemistry*, 34, 451–465.
- Jain, M., Garg, V. K., & Kadirvelu, K. (2009). Equilibrium and kinetic studies for sequestration of Cr(VI) from simulated wastewater using sunflower waste biomass. *Journal of Hazardous Materials*, 171, 328–334.
- Jaina, M., Garga, V. K., & Kadirvelu, K. (2009). Chromium(VI) removal from aqueous system using *Helianthus annuus* (sunflower) stem waste. *Journal of Hazardous Materials*, 162, 365–372.
- Khan, T. A., Mukhlif, A. A., Khan, E. A., & Sharma, D. K. (2016). Isotherm and kinetics modeling of Pb(II) and Cd(II) adsorptive uptake from aqueous solution by chemically modified green algal biomass. *Model Earth Syst. Environ*, 2, 117.
- Khoubestani, R. S., Mirghaffari, N., & Farhadian, O. (2015). Removal of three and hexavalent chromium from aqueous solutions using a microalgae biomass-derived biosorbent. *Environmental Progress & Sustainable Energy*, 34, 949–956.
- Kuppusamy, S., Thavamani, P., Megharaj, M., Venkateswarlu, K., Lee, Y. B., & Naidu, R. (2016). Potential of *Melaleuca diosmifolia* leaf as a low-cost adsorbent for hexavalent chromium removal from contaminated water bodies. *Process Safety and Environmental Protection*, 100, 173–182.
- Lagergren, S. (1898). About the theory of so-called adsorption of soluble substances, Zur theorie der sogenannten adsorption gelster stoffe. *Kungliga Svenska Vetenskapsakademiens, Handlingar; Band*, 24(1898), 1–39.
- Langmuir, I. (1918). The adsorption of gases on plane surfaces of glass, mica and platinum. *Journal of the American Chemical Society*, 40, 1361–1368.
- Lodeiro, P., Barriada, J. L., Herrero, R., & Sastre de Vicente, M. E. (2006). The marine macroalga *Cystoseira baccata* as biosorbent for cadmium(II) and lead(II) removal: kinetic and equilibrium studies. *Environmental Pollution*, 142, 264–273.
- Ly, L., Chen, N., Feng, C., Zhang, J., & Li, M. (2017). Heavy metal ions removal from aqueous solution by xanthate-modified cross-linked magnetic chitosan/poly(vinyl alcohol) particles. *Royal Society of Chemistry Advances*, 7, 27992–28000.
- Ma, J., Qin, G., Zhang, Y., Sun, J., Wang, S., & Jiang, L. (2018). Heavy metal removal from aqueous solutions by calcium silicate powder from waste coal fly-ash. *Journal of Cleaner Production*, 182, 776–782.
- Mahmoud, M. A. (2015). Thermodynamics and kinetics studies of Mn (II) removal from aqueous solution onto powder corn cobs (PCC). *Chromatography Separation Techniques*, 6(7), 301.
- Mahmud, H. N. M. E., Huq, A. K. O., & Yahya, R. B. (2016). The removal of heavy metal ions from wastewater/aqueous solution using polypyrrole-based adsorbents: a review. *Royal Society of Chemistry Advances*, 6, 14778–14791.
- Mondal, N. K., & Basu, S. (2019). Potentiality of waste human hair towards removal of chromium(VI) from solution: kinetic and equilibrium studies. *Applied Water Science*, 9(49).
- Muthukumar, K., & Beulah, S. (2011). Removal of chromium (VI) from wastewater using chemically activated *Syzygium jambolanum* nut carbon by batch studies. *Procedia Environmental Sciences, Urban Environmental Pollution 2010*, 4, 266–280.
- Nakkeeran, E., & Selvaraju, N. (2017). Biosorption of chromium (VI) in aqueous solutions by chemically modified Strychnine tree fruit shell. *International Journal of Phytoremediation*, 19(12), 1065–1076.
- Nameni, M., Moghadam, M. R. A., & Arami, M. (2008). Adsorption of hexavalent chromium from aqueous solutions by wheat bran. *International Journal of Environmental Science & Technology*, 5(2), 161–168.
- Nasseh, N., Taghavi, L., Barikbin, B., & Harifi-Mood, A. R. (2017). The removal of Cr(VI) from aqueous solution by almond green hull waste material: kinetic and equilibrium studies. *Journal of Water Reuse and Desalination*, 7, 449–460.
- Niazi, L., Lashanizadegan, A., & Sharififard, H. (2018). Chestnut oak shells activated carbon: Preparation, characterization and application for Cr (VI) removal from dilute aqueous solutions. *Journal of Cleaner Production*, 185, 554–561.
- Olguin, M. T., López-González, H., & Serrano-Gómez, J. (2013). Hexavalent chromium removal from aqueous solutions by Fe-modified peanut husk. *Water Air Soil Pollution*, 224(1654).
- Pandey, P. K., Sharma, S. K., & Sambhi, S. S. (2010). Kinetics and equilibrium study of chromium adsorption on zeoliteNaX. *International Journal of Environmental Science & Technology*, 7, 395–404.
- Parlayıcı, Ş., & Pehlivan, E. (2019). Comparative study of Cr(VI) removal by bio-waste adsorbents: equilibrium, kinetics, and thermodynamic. *Journal of Analytical Science and Technology*, 10(15).
- Pourfadakari, S., Jorfi, S., Ahmadi, M., & Takdastan, A. (2017). Experimental data on adsorption of Cr(VI) from aqueous solution using nanosized cellulose fibers obtained from rice husk. *Data in Brief*, 15, 887–895.
- Rangabhashiyam, S., & Selvaraju, N. (2015a). Evaluation of the biosorption potential of a novel *Caryota urens* inflorescence waste biomass for the removal of hexavalent chromium from

- aqueous solutions. *Journal of the Taiwan Institute of Chemical Engineers*, 47, 59–70.
- Rangabhashiyam, S., & Selvaraju, N. (2015b). Efficacy of unmodified and chemically modified *Swietenia mahagoni* shells for the removal of hexavalent chromium from simulated wastewater. *Journal of Molecular Liquids*, 209, 487–497.
- Saha, R., Mukherjee, K., Saha, I., Ghosh, A., Ghosh, S. K., & Saha, B. (2013). Removal of hexavalent chromium from water by adsorption on mosambi (*Citrus limetta*) peel. *Research on Chemical Intermediates*, 39(5), 2245–2257.
- Sari, A., & Tuzen, M. (2008). Biosorption of total chromium from aqueous solution by red algae (*Ceramium virgatum*): Equilibrium, kinetic and thermodynamic studies. *Journal of Hazardous Materials*, 160, 349–355.
- Sathish, T., Viniithkumar, N. V., Dharani, G., & Kirubakaran, R. (2015). Efficacy of mangrove leaf powder for bioremediation of chromium (VI) from aqueous solutions: kinetic and thermodynamic evaluation. *Applied Water Science*, 5, 153–160.
- Sharma, D. C., & Forster, C. F. (1994). A preliminary examination into the adsorption of hexavalent chromium using low-cost adsorbents. *Bioresource Technology*, 47, 257–264.
- Shukla, S. S., Yu, L. J., Dorris, K. L., & Shukla, A. (2005). Removal of nickel from aqueous solutions by sawdust. *Journal of Hazardous Materials*, 121, 243–246.
- Singh, K. K., Rastogi, R., & Hasan, S. H. (2005). Removal of Cr(VI) from wastewater using rice bran. *Journal of Colloid and Interface Science*, 290, 61–68.
- Singha, B., & Das, S. K. (2011). Biosorption of Cr(VI) ions from aqueous solutions: kinetics, equilibrium, thermodynamics and desorption studies. *Colloids and Surfaces B: Biointerfaces*, 84, 221–232.
- Singha, B., Naiya, T. K., Bhattacharya, A. K., & Das, S. K. (2011). Cr(VI) ions removal from aqueous solutions using natural adsorbents – FTIR studies. *Journal of Environmental Protection*, 02, 729–735.
- Sugashini, S., & Begum, K. M. M. S. (2013). Optimization using central composite design (CCD) for the biosorption of Cr(VI) ions by cross linked chitosan carbonized rice husk (CCACR). *Clean Technology and Environmental Policy*, 15, 293–302.
- Vinodhini, V., & Das, N. (2010). Relevant approach to assess the performance of sawdust as adsorbent of chromium (VI) ions from aqueous solutions. *International Journal of Environmental Science & Technology*, 7, 85–92.
- Weber, W. J., & Morris, J. C. (1963). Kinetics of adsorption of carbon from solution. *Journal of the Sanitary Engineering Division. American Society of Civil Engineering*, 89, 31–60.
- Yang, L., & Chen, J. P. (2008). Biosorption of hexavalent chromium onto raw and chemically modified *Sargassum* sp. *Bioresource Technology*, 99, 297–307.
- Yogeshwaran, V., & Ak, P. (2017). Removal of hexavalent chromium (Cr⁶⁺) using different natural adsorbents - a review. *Journal of Chromatography & Separation Techniques*, 8, 1–6.

Publisher's note Springer Nature remains neutral with regard to jurisdictional claims in published maps and institutional affiliations.